J|A|C|S
COMMUNICATIONS

Published on Web 03/24/2007

Mesoporous Au/TiO_2 Nanocomposites with Enhanced Photocatalytic Activity

Hexing Li,*,† Zhenfeng Bian,† Jian Zhu,† Yuning Huo,† Hui Li,† and Yunfeng Lu*,‡

Department of Chemistry, Shanghai Normal University, Shanghai 200234, China, and Chemical & Biomolecular Engineering Department, University of California, Los Angeles, California 90095

Received December 19, 2006; E-mail: hexing-Li@shnu.edu.cn; luucla@ucla.edu

Mesoporous materials with tunable pore structure and tailored framework composition are of great interest for broad applications ranging from adsorbent, separation, catalyst, energy storage and conversion, to biological uses.[1] Among this material family, mesoporous titania is of particular interest since the semiconductive framework is photoactive while mesoporous channels offer larger surface area and enhanced accessibility. Such a unique combination provides a new platform for design and fabrication of novel photoactive materials and devices, such as high-efficiency photocatalyst and photovoltaic.[2] To date, limited by titania's low quantum efficiency and high band gap (3.0 ~ 3.2 eV, located at the ultraviolet (UV) wavelength range),[3] utilizing mesoporous titania as highly active photocatalyst, however, remains challenging. Possible strategies toward this intrinsic limitation include doping titania with inorganic or metallic species, such as ions and clusters, or photosensitizing titania with organic dyes that are often efficient but unstable.[4]

This work reports the synthesis of highly active mesoporous titania photocatalyst by embedding gold nanoparticles, a highly stable inorganic photosensitizer, homogenously within the framework. Controlling the nanoparticle size affords tunable quantum effect, enhanced visible-light adsorption, and significantly enhanced photocatalytic activity. Although metal nanoparticles have been incorporated into mesoporous materials previously,[5,6] this was achieved by impregnating metal precursor within a preformed mesoporous scaffold and subsequent reducing reaction. The formed nanoparticles were often poorly controlled in size and preferably located within the pore channels rather than embedded within the framework.

To homogenously embed gold nanoparticles within the titania framework, we utilized a multicomponent assembly approach, where surfactant, titania, and gold building clusters were cooperatively assembled in an one-step process (see Supporting Information for details). Briefly, Pluronic surfactant P123, $TiCl_4$, $Ti(OBu)_4$, and $AuCl_3$ were mixed in ethanol. Casting the mixture followed by an aging process resulted in homogeneous mesostructured nanocomposites. Calcination removed P123 and created crystalline mesoporous TiO_2 networks embedding gold nanoparticles. Figure 1a and 1b respectively shows a transmission electron micrograph (TEM) of a hexagonal mesoporous TiO_2 with 0.5 mol % Au along the (100) and (110) plane, indicating an average wall thickness of 5.0 nm. Selective area electron diffraction (SAED, inset b) shows well-resolved diffraction cycles indicative of a highly crystalline TiO_2 framework. Although energy disperse X-ray spectra (EDS) confirms the presence of Au, no Au nanoparticles could be observed by TEM. Nevertheless, X-ray photoelectron spectrum (XPS) (Figure S3) shows binding energies (BE) of $Au_{4f7/2}$ at 83.4 and $Au_{4f5/2}$ at 87.0 eV, which are significantly different from $Au^{+}{}_{4f7/2}$ (84.6 eV) and $Au^{3+}{}_{4f7/2}$ (87.0 eV) but similar to $Au^{0}{}_{4f7/2}$ (84.0 eV).[4,7] The XPS

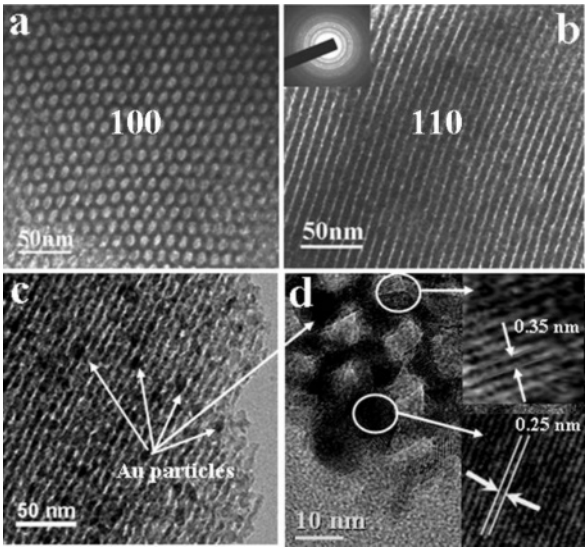

Figure 1. Representative TEM images of 0.5 mol % Au/TiO_2 along (a) [100] and (b) [110] plane, (c) 1.0 mol % Au/TiO_2 along [110] plane, and (d) high-resolution image of 2.0 mol % Au/TiO_2.

result suggests that the Au species are present in the metallic state and the negative shift of $Au^{0}{}_{4f7/2}$ (0.6 eV) indicates strong interactions between Au and the TiO_2 framework. Furthermore, in comparison with the mesoporous TiO_2 impregnated 0.5 mol % Au (Figure S4), the above studies indicate the formation of small, well-dispersed Au nanoparticles preferably within the framework. Increasing Au content results in larger nanoparticles. For example, TEM image (Figure 1c) of mesoporous TiO_2 containing 1.0 mol % Au clearly shows nanoparticles with a diameter 12~15 nm in the pore channels. Both nanoparticle and framework are highly crystallized as evidenced from the well resolved Au(111) (0.25 nm) and TiO_2(101) (0.36 nm) crystalline lattices as shown in Figure 1d.

Low-angle XRD patterns of the nanocomposites (Figure S5) reveals well resolved (100), (110), and (200) reflections confirming an ordered 2D-hexagonal mesostructure.[8] The gradually decreasing peak intensity with increasing Au content suggests a decreasing long-range order. Nevertheless, they display similar nitrogen sorption isotherms with narrow pore-size distributions centered at about 6.0~6.8 nm (Figure S6), which is typical for surfactant-templated mesoporous materials. Detailed pore structure information is listed in Table S1. The pore volume and surface area are decreased with increasing Au content, which is consistent with a weaker TiO_2 framework structure owing to the intrusion of nanoparticles and with the presence of larger nanoparticles in their pore channels. Wide-angle XRD (Figure S7) shows intense (101), (004), and (200) reflections of an anatase structure.[9] Mesoporous TiO_2 with a low Au content (e.g., <0.5%) does not exhibit any Au characteristic diffraction, further confirming the small nanoparticle

† Shanghai Normal University.
‡ University of California.

10.1021/ja069113u CCC: $37.00

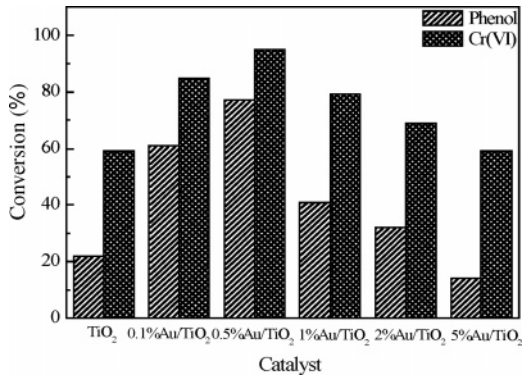

Figure 2. Photocatalytic activity of Au/titania nanocomposites containing 0 to 5% Au in phenol-oxidation and chromium-reduction reactions.

size. Characteristic Au diffractions with increasing intensity and narrowing half-peak width are observed with increasing Au content, indicating an increasing particle size. The Au crystallite size in the 2.0 mol % Au/TiO_2 was estimated as 12 nm from the Scherrer equation, consistent with the TEM observation.

On the basis of the above results, we believe the formation of these nanocomposites involves assembly of inorganic building clusters and surfactant-forming ordered lyotropic liquid crystalline phase[10] (see Scheme S1). FTIR spectra (Figure S8) demonstrates that, besides a broad absorbance peak in the range from 3100 to 3450 cm^{-1} and a strong absorbance peak around 1610 cm^{-1} attributing to the vibrations of the surface-adsorbed H_2O and Ti−OH bonds,[11] a peak characteristic of Ti−O−Au bond is also observed around 1410 cm^{-1}.[12] This observation confirms co-assembly of the titania and gold building clusters into homogeneous nanocomposites. Subsequent calcination removes surfactant and decomposes −Ti−O−Au− bonds, creating mesoporous TiO_2 and Au nanoparticles. A low Au content results in smaller nanoparticles that are homogeneously embedded within the framework, while a high gold content generates larger particles that are expelled from framework to the pore channels.

These unique nanocomposites show significantly improved photocatalytic activities. Figure 2 compares the conversion of phenol oxidation and chromium reduction catalyzed by the mesoporous nanocomposites with different Au loadings. Two representative conversion curves were shown in Figure S9. When the reactions were conducted under dark condition, no reactions were observed even after 6 h, indicating the really photocatalytic reactions. The conversion of phenol oxidation and chromium reduction continuously increases from 22% to 95% when Au content is increased from 0 to 0.5%. A near three-time improvement in phenol decomposition is achieved when 0.5% of Au was doped, unambiguously suggesting a significantly improved photocatalytic activity. Further increasing Au content, however, decreases catalytic activity.

As the ^{13}C CP-MAS NMR spectra confirm that both the undoped TiO_2 and the Au/TiO_2 contain no significant carbon species (Figure S1), such improved photocatalytic activities may be attributed to the enhanced light absorption and improved quantum efficiency. The UV−visible DRS spectra (Figure S10) demonstrates a significantly enhanced absorption in the visible range (500∼600 nm) owing to the plasmon resonance effect.[13] The absorbance intensified and red-shifted with increasing Au loading, which is consistent with the formation of more and bigger particles.[14] The enhanced light absorption can therefore provide more photocharges needed for the photocatalytic reactions. Figure S11 shows the Raman spectra of the nanocomposites with different Au loadings. The absorption at 146 cm^{-1} indicates an anatase crystalline framework structure.[15] The absorption becomes broader and weaker and shifts positively in position by 8 cm^{-1} when the Au content is increased from 0.1 to 0.5%, suggesting increased crystalline defects within the framework.[15] Such defects may favor capturing photoelectrons and inhibiting charge recombination. Meanwhile, Au nanoparticles embedded within the framework may also serve as an electron conductor, which facilitates photoelectron transfer to pore surface and further reduce the probability of charge recombination.[5] When Au content is further increased from 0.5 to 5.0%, no significant effect on the Raman peak position was observed. This observation is consistent with TEM and XRD observations showing the formation of large nanoparticles within the pore channels (see Figure 1c). Rather than facilitate charge transport and reduce charge recombination, the large nanoparticles may act as the centers of electron−hole recombination[16] and reduce quantum efficiency. Moreover, the presence of a large number of nanoparticles within the pore channels may also slow down mass transport and reduce the reaction rate. These factors may account for the observed decreasing photocatalytic activity at a higher Au content (e.g., >0.5%).

In summary, we have demonstrated the synthesis of highly active mesoporous Au/TiO_2 nanocomposites with significantly improved photocatalytic activity. We believe that enhanced light absorption and improved quantum efficiency are the main factors leading to the improved photocatalytic activity. This work provides a new pathway to design and fabricate novel photoactive materials for catalyst and other applications.

Acknowledgment. This work was supported by the National Natural Science Foundation of China (2005CCA01100) and the Natural Science Foundation of Shanghai Science (06JC14060, T0402).

Supporting Information Available: Preparation and characterization (XRD, XPS, Raman, FTIR, NMR, UV−visible diffuse reflectance spectra, nitrogen sorption, TGA-DTA, photocatalytic activity test) of Au/TiO_2 nanocomposites. This material is available free of charge via the Internet at http://pubs.acs.org.

References

(1) (a) Beck, J. S.; Vartuli, J. C. *Curr. Opin. Solid State Mater. Sci.* **1996**, *1*, 76. (b) Davis, M. E. *Nature* **2002**, *417*, 813. (c) Liu A. M.; Hidajat, K.; Kawi, S.; Zhao, D. Y. *Chem. Commun.* **2000**, 1145.
(2) Yu, J. C.; Wang, X. C.; Ho, W. *Adv. Funct. Mater.* **2004**, *14*, 1178.
(3) Asahi, R.; Morikawa, T.; Ohwaki, T.; Taga, Y. *Science* **2001**, *293*, 269.
(4) (a) Choi, W. Y.; Hoffmann, M. R. *J. Phys. Chem.* **1994**, *98*, 13669. (b) Li, F. B.; Li, X. Z. *Appl. Catal., A* **2002**, *228*, 15. (c) Arabatzis, I. M.; Stergiopoulos, T.; Andreeva, D.; Kitova, S.; Neophytides, S. G.; Falaras, P. *J. Catal.* **2003**, *220*, 127. (d) Sonawane, R. S.; Dongare, M. K. *J. Mol. Catal. A: Chem.* **2006**, *243*, 68.
(5) (a) Cheng, S.; Wei, Y.; Feng, Q. W.; Pang, J. B.; Jansen, S. A.; Yin, R.; Ong, K. *Chem. Mater.* **2003**, *15*, 1560. (b) Lu, G. M.; Zhao, R.; Qian, G.; Qi, Y. X. *Catal. Lett.* **2004**, *97*, 115. (c) Sreethawong, T.; Yoshikawa, S. *Catal. Commun.* **2005**, *6*, 661. (d) Idakiev, V.; Tabakova, T.; Naydenov, A.; Yuan, Z. Y.; Su, B. L. *Appl. Catal. B* **2006**, *63*, 178.
(6) Wang, X. C.; Yu, J. C.; Ho, C.; Mak, A. C. *Chem. Commun.* **2005**, 2262.
(7) Mottet, C.; Treglia, G.; Legrand, B. *Surf. Sci.* **1996**, *675*, 352.
(8) Tian, B. Z.; Yang, H. F.; Liu, X. Y.; Xie, S. H.; Yu, C. Z.; Fan, J.; Tu, B.; Zhao, D. Y. *Chem. Commun.* **2002**, 1824.
(9) Yu, J. C.; Li, G. S.; Leung, C.; Zhang, Z. D. *Chem. Commun.* **2006**, 2717.
(10) Firouzi, A.; Kumar, D.; Bull, L. M.; Besier, T.; Sieger, P.; Huo, Q.; Margolese, D.; Stucky, G. D.; Chmelka, B. F. *Science* **1995**, *267*, 1138.
(11) Li, H. X.; Li, J. X.; Huo, Y. N. *J. Phys. Chem. B* **2006**, *110*, 1559.
(12) Mihaylov, M. Y.; Fierro-Gonzalez, J. C.; Kno1zinger, H.; Gates, B. C.; Hadjiivanov, K. I. *J. Phys. Chem. B* **2006**, *110*, 7695.
(13) Yonezawa, T.; Matsune, H.; Kunitake, T. *Chem. Mater.* **1999**, *11*, 33.
(14) Jensen, T. R.; Duyne, R. P. V. *J. Phys. Chem. B* **1999**, *103*, 2394.
(15) Parker, J. C.; Siegel, R. W. *Appl. Phys. Lett.* **1990**, *57*, 943.
(16) Subramanian, V.; Wolf, E. E.; Kamat, P. V. *Langmuir* **2003**, *19*, 469.

JA069113U